



OPEN

# Probing impact on magnetic behavior of cobalt layer grown on thick MoS<sub>2</sub> layer

Zainab Hussain<sup>1✉</sup>, Shashikant P. Patole<sup>2✉</sup>, Shoyebmohamad F. Shaikh<sup>3</sup>, P. E. Lokhande<sup>4</sup> & Habib M. Pathan<sup>1</sup>

Understanding the metal-semiconductor heterostructure interface is crucial for the development of spintronic devices. One of the prospective candidates and extensively studied semiconductors is molybdenum disulfide (MoS<sub>2</sub>). Herein, utilizing Kerr microscopy, we investigated the impact of thick MoS<sub>2</sub> on the magnetic properties of the 10 nm Co layer. A comparative study on Co/MoS<sub>2</sub> and Co/Si shows that coercivity increased by 77% and the Kerr signal decreased by 26% compared to Co grown on Si substrate. In addition, the Co domain structure significantly changed when grown on MoS<sub>2</sub>. The plausible reason for the observed magnetic behavior can be that the Co interacts differently at the interface of MoS<sub>2</sub> as compared to Si. Therefore, our studies investigate the interfacial effect on the magnetic properties of Co grown on thick MoS<sub>2</sub> layer. Furthermore, our results will help in developing next-generation spintronic devices.

State-of-the-art spintronic devices rely substantially on recent advances in understanding the metal-semiconductor heterostructure interface. The last few decades have witnessed unprecedented advancement in using 2D transition metal dichalcogenides (TMDC) materials as semiconductors in various next-generation storage, sensors, and flexible electronics devices<sup>1</sup>. 2D TMDC materials have fascinating properties like direct band-gap at monolayers, flexibility, and tunable optical and electronic properties<sup>1,2</sup>. On the other hand, heterostructures composed of ferromagnetic and TMDC materials have great importance as they provide spin-orbit torque and consequently can be utilized in magnetic tunnel junction (MTJ) for charge-to-spin conversion<sup>2</sup>. Heavy materials, like Pt, Ta, etc., are typically used as spin torque due to their large spin-orbit coupling<sup>3</sup>. However, heavy metal/ferromagnetic junctions cannot be efficiently utilized for out-of-plane magnetic anisotropy magnetic tunnel junctions, and their charge-spin conversion efficiency is less<sup>2,3</sup>. Nevertheless, TMDC/FM heterostructure can be utilized as efficient charge-spin conversion for out-of-plane magnetic MTJ. Besides this, recent advancement shows that TMDC materials have great potential in low-powered spintronic devices because of the higher spin-orbit torque efficiency<sup>3,4</sup>.

The most widely studied 2D TMDC material is MoS<sub>2</sub>. Recently, various experimental evidence shows that MoS<sub>2</sub> not only contributes in inducing the perpendicular anisotropy but also aids in inducing in-plane anisotropy and coercivity enhancement<sup>5-8</sup>. Even experimental and theoretical reports suggest that hybridization and low symmetry at the interface can lead to various exotic magnetic behaviors<sup>9,10</sup>. Currently, in literature, there have been reports on FM layer/monolayer MoS<sub>2</sub> heterostructure<sup>5,6,11,12</sup>. Furthermore, in the past few years, scientists have extensively studied and explored monolayer and multilayer 2D TMDC/FM heterostructures<sup>11,13-16</sup>. In a few such studies, one can find the investigation of Fe deposited on MoS<sub>2</sub>, which suggests that Fe does not react or bond with MoS<sub>2</sub> and aggregates<sup>11,17-19</sup>. Nonetheless, a study on the Co grown on monolayer MoS<sub>2</sub> shows that Co forms a covalent bond, and the spin magnetic moment also decreases<sup>11</sup>. This hybridization leads to the induced magnetic anisotropy in the Co layer<sup>11</sup>. Further, a theoretical report shows the hybridization of Co and S at the interface of Co/MoS<sub>2</sub> hetero-junctions<sup>20</sup>. Therefore, this suggests that one can tailor the magnetic behavior of the suitable FM layer, i.e., the Co layer, with the proximity of the MoS<sub>2</sub> layer.

Apart from this, the interfacial effect on magnetic properties of the FM layer grown on the thick MoS<sub>2</sub> layer has received little attention, even though the scalability of the 2D TMDC layer is essential for application purposes. Contrarily, instead of utilizing techniques such as mechanical exfoliation or chemical vapor deposition

<sup>1</sup>Advanced Physics Laboratory, Department of Physics, Savitribai Phule Pune University, Pune 411007, India. <sup>2</sup>Department of Physics, Khalifa University of Science and Technology, P.O. Box 127788, Abu Dhabi, United Arab Emirates. <sup>3</sup>Department of Chemistry, College of Science, King Saud University, P.O. Box 2455, 11451 Riyadh, Saudi Arabia. <sup>4</sup>Departamento de Mecánica, Facultad de Ingeniería, Universidad Tecnológica Metropolitana, Santiago, Chile. ✉email: zaineb92@gmail.com; shashikant.patole@ku.ac.ae

to fabricate 2D TMDC layers, physical vapor deposition (sputtering) or direct sulfurization can produce homogeneous large-scale thick 2D TMDC layer<sup>21,22</sup>. It should also be noted that the wettability of the thick MoS<sub>2</sub> increases with thickness as comparable to monolayer<sup>23</sup>. Hence, it is essential to investigate the interfacial effect of thick MoS<sub>2</sub> on the magnetic properties of the FM layer. Consequently, it would be interesting to study the impact of the thick MoS<sub>2</sub> interface on the Co layer. Therefore, our work provides an understanding of the impact on the magnetic behavior of the Co grown on the thick MoS<sub>2</sub> layer prepared by direct sulfurization technique. Magneto-optical Kerr microscopy is employed in the present work to get valuable insights into magnetic behavior.

## Experimental

The MoS<sub>2</sub> layer was prepared by sulfurization of commercially purchased Mo thin film deposited on glass substrate. The sulfurization was carried in tube type furnace by annealing at 450°C temperature with 95% of argon and 5% of H<sub>2</sub>S gases for 1 hour. On other hand, the deposition of the Co layer on as-prepared MoS<sub>2</sub> was carried out by using a DC magnetron sputtering (dcMS) system at the rate of 0.2Å per second at 50 watt. A capping layer of TiN ( $\approx$  3nm) was deposited on the top of Co layer to avoid oxidation. Prior to the deposition, the as-prepared MoS<sub>2</sub> sample was cleaned by RF biasing at 50 watt for 10 minutes for the removal of the contamination on the MoS<sub>2</sub>. Further, to compare the magnetic properties, Si substrate was mounted adjacent to MoS<sub>2</sub>. Thus, the deposition conditions were same for both the samples. The Raman spectroscopy was carried on the as-prepared sample by using cyan laser. Also scanning electron microscopy (SEM) and field emission scanning electron microscopy along with energy dispersive spectroscopy (EDS) were performed on the samples. Moreover, atomic force microscopy (AFM) in tapping mode was performed to study the topography of the as-deposited samples. Imaging of the magnetic domains and the study of the magnetic anisotropy in the films was conducted by magneto-optical Kerr microscopy (M/s Evico Magnetics, Germany). Hysteresis loops were obtained by deriving the magnetization signal from the average domain image intensity.

## Results and discussions

The MoS<sub>2</sub> layer was prepared by sulfurizing the sputtered Mo thin film of around  $780 \pm 39 \mu\text{m}$  thick (confirmed by the SEM image in Fig. 1a). The sulfurization process is illustrated in Fig. 1b. It should be noted that in literature, large-scale MoS<sub>2</sub> can be fabricated by various techniques such as sputtering, chemical vapor deposition, etc.<sup>24</sup>. However, sulfurization using sulfurization agent H<sub>2</sub>S gas is a simple and effective technique<sup>24,25</sup>. Consequently, we have selected H<sub>2</sub>S gas for the sulfurization of the MoS<sub>2</sub> followed by deposition of Co layer of 10 nm and capped with TiN. To elucidate the structural uniformity at the interface and for chemical characterization, we have performed field emission scanning microscopy (FE-SEM) along with energy dispersive spectroscopy (EDS) on the Co/MoS<sub>2</sub> heterostructure. Figure 1c displays the FESEM micrograph Co/MoS<sub>2</sub> heterostructure indicating uniform and compact structure. Further, two contrast (structure) is visible, indicating two distinct layers. It probably indicates that the top Mo layers are sulfurized only. This observation is confirmed by grazing angle

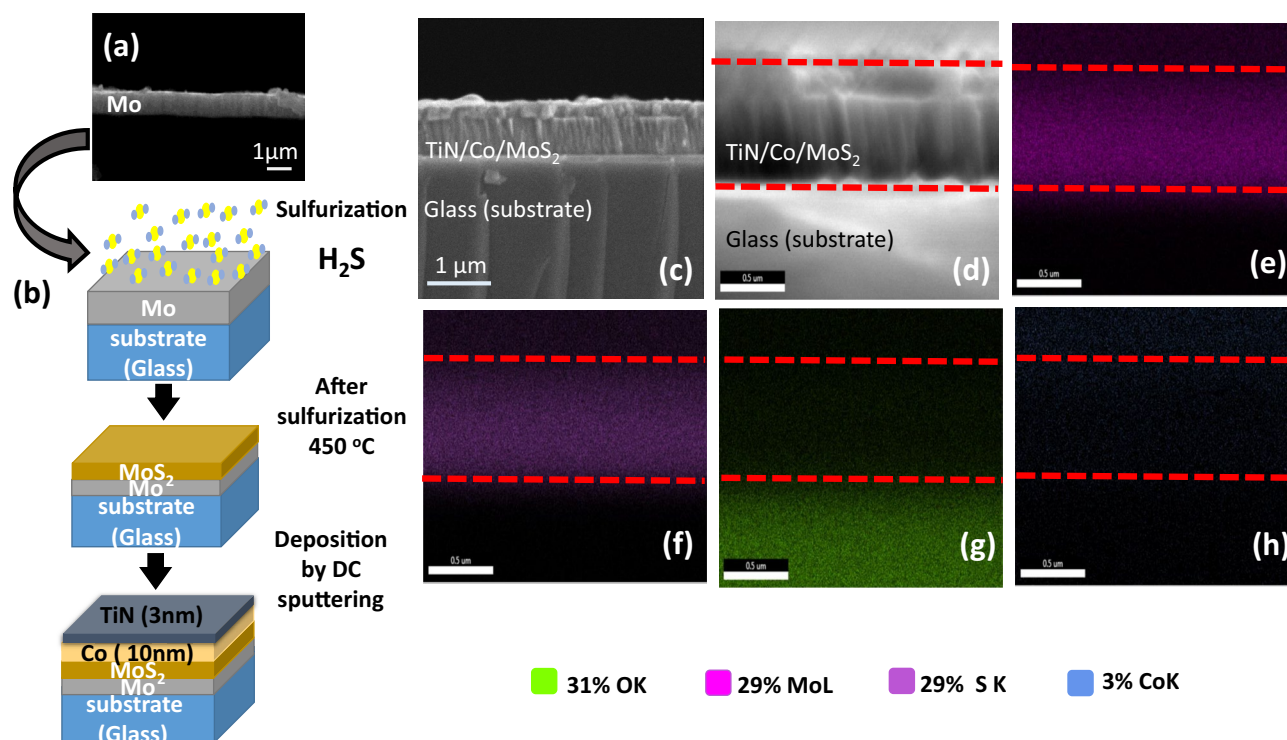


**Figure 1.** (a) Displays the SEM image of Mo thin film. (b) Illustrate the process of the sulfurization and deposition. (c) Displays the FE-SEM image of Co/MoS<sub>2</sub> (d–h), Display the EDS images.

X-ray diffraction measurements (supplementary). The corresponding EDS mapping is displayed in Fig. 1d–h, confirming the deposition of different layers like Co and MoS<sub>2</sub>. Although from the EDS contrast image, it is difficult to distinguish the distribution of Co and S precisely since the EDS resolution is limited by 1 micron. However, one can identify the presence of elements like Mo, Co, O, and S. The formation of MoS<sub>2</sub> is confirmed by the Raman spectra in Fig. 2. One can clearly see the two characteristic peaks corresponding to in-plane ( $E_{2g}^1$ ) and out-of-plane ( $A_{1g}$ ) vibrational modes at 381.8 cm<sup>-1</sup> and 407.5 cm<sup>-1</sup> respectively. The separation between two peaks is  $\approx 25$  cm<sup>-1</sup> indicating the bulk nature of MoS<sub>2</sub> layer<sup>1</sup>. Besides this, the AFM is performed to study the morphology and surface of the as-deposited samples. Analyzing the topography of both samples by AFM can be helpful in providing information regarding the interface. Figure 3 shows the AFM images taken at different resolutions for TiN/Co/Si and TiN/Co/Si, respectively. The frames below show the 3-D image and the line profile for both samples. It is observed that the root mean square (RMS) roughness for both the samples are different, i.e., 0.64 nm for TiN/Co/Si and 15.1 nm for TiN/Co/MoS<sub>2</sub>. It indicates that the roughness significantly increased when Co has grown MoS<sub>2</sub> underlayer. Moreover, the grain size of the surface calculated by the line profile is 45  $\pm$  8 nm for TiN/Co/Si, while 90  $\pm$  11 nm for TiN/Co/MoS<sub>2</sub>. Thus, the AFM study indicated that the Co grows and interacts differently on the interface of the MoS<sub>2</sub> as compared to the Si; this leads to modification in the morphology in Co/MoS<sub>2</sub>.

In order to investigate the magnetic behavior of as-deposited Co/MoS<sub>2</sub> heterostructure, we have performed Kerr microscopy. For comparison of magnetic properties, we have compared with the Co layer grown on the silicon substrate. The magnetic hysteresis loops measured along the magnetic domain structure for both the samples Co/Si and Co/MoS<sub>2</sub> is displayed in Fig. 4. One can clearly observe the increase in coercivity by 77% and a decrease in Kerr signal by 26% as compared to the Co/Si sample. The reduction in the Kerr signal signifies that

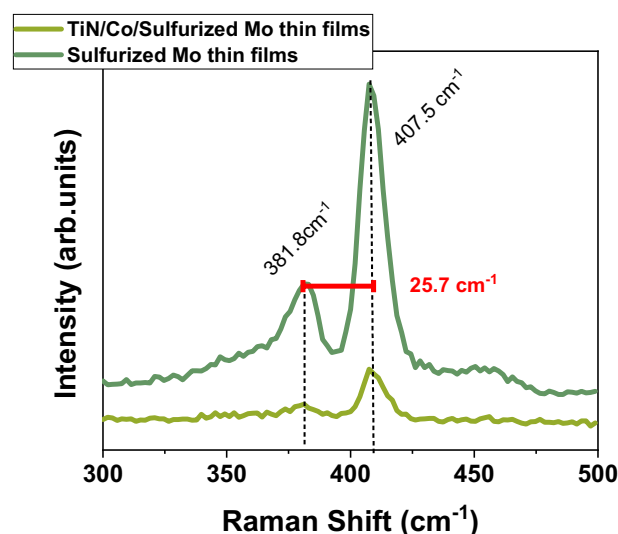


**Figure 2.** Displays the Raman spectra before and after the deposition of Co layer. One can clearly see the presence of two characteristic peaks confirming the formation of MoS<sub>2</sub>.

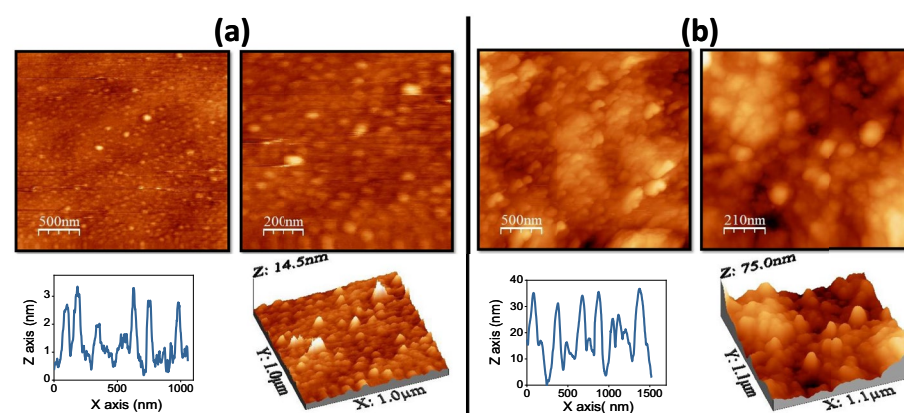


**Figure 3.** Displays the AFM images of the (a) TiN/Co/Si (b) TiN/Co/MoS<sub>2</sub> at different resolutions. Below frames, shows the line profiles and 3-D image of the TiN/Co/Si and TiN/Co/MoS<sub>2</sub> respectively.

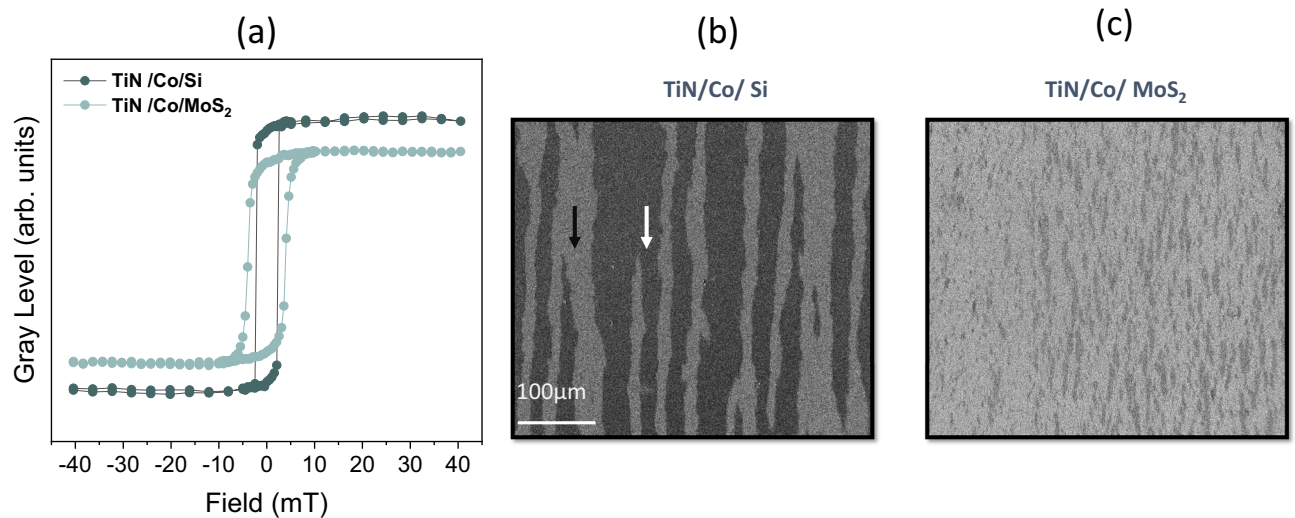


**Figure 4.** Displays the hysteresis loop for Co/Si and Co/MoS<sub>2</sub> and the corresponding domain structure captured at remanence state.

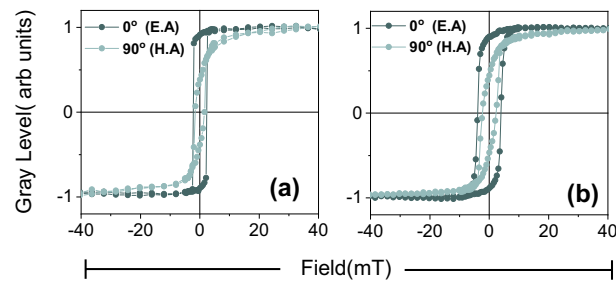


**Figure 5.** Displays the magnetic hysteresis loops measured along easy axis and hard axis which is designated as 0° and 90° for (a) TiN/Co/Si and (b) TiN/Co/MoS<sub>2</sub> respectively.

the contribution from the magnetic moment is decreased<sup>18,26</sup>. It could be due to roughness or inhomogeneous microstructure at the interface. Further, increasing the coercivity indicates an increase in the pinning center due to inhomogeneity or roughness at the interface. To get deeper insights into the magnetic behavior, the magnetic domain structure was captured along the remanence state by applying a decreasing A.C. field along the easy axis of magnetization. From Fig. 4, a noteworthy difference in domain structure can be observed for both samples. The fine domains are observed in Co/MoS<sub>2</sub>; contrarily, large domains are observed for Co/Si. The observation of fine magnetic domain for Co/MoS<sub>2</sub> can be attributed to the fact that the magnetic domains often split into smaller domains when the pinning centers are increased in order to reduce the magneto-static energy<sup>27</sup>. Moreover, domain structure corroborates the observation of increased coercivity in Co/MoS<sub>2</sub> compared with Co/Si.

In an effort to study the in-plane magnetic anisotropy in both the samples. The hysteresis loops were measured along the in-plane azimuthal angles. Figure 5 displays the hysteresis loop measured along an easy axis (E.A.) and hard axis (H.A.), which is designated as 0° and 90°. Apparently, both the samples, i.e., Co/Si and Co/MoS<sub>2</sub>, possess magnetic anisotropy. Usually, the polycrystalline Co thin film possesses in-plane magnetic anisotropy due to various causes<sup>28</sup>. From Fig. 5, it is clear that MoS<sub>2</sub> does not contribute much to the magnetic anisotropy. For comparison, the coercivity values ( $H_C$ ) and squareness ( $M_r/M_s$ ) for 0° and 90° shown in Table 1. One clearly observed that the  $H_C$  is more for the 0° and 90° in Co/MoS<sub>2</sub> as compared to Co/Si.

Sample	E.A $H_C$ (mT)	H.A $H_C$ (mT)	$M_r/M_s$
TiN/Co/Si	2.2	1.5	0.38
TiN/Co/MoS <sub>2</sub>	3.9	2.2	0.45

**Table 1.** Parameters obtained from hysteresis loops ( in Fig. 5) is shown below in table.



## Conclusions

The impact on the magnetic properties of Co grown on thick MoS<sub>2</sub> under layer is investigated with magneto-optical Kerr microscopy. The results are compared with the conventional Co thin films grown on Si substrate. Results show that Co/MoS<sub>2</sub>, coercivity increased by 77%, and the Kerr signal decreased by 26% compared to Co grown on Si substrate. In addition, the Co domain structure significantly changed when grown on MoS<sub>2</sub>. The plausible reason for the observed magnetic behavior can be that the Co interacts differently at the interface of MoS<sub>2</sub>. This leads to a significant change in the morphology and magnetic behavior. Further, this aspect needs to be explored in more detail. Experiments like X-ray photoelectron spectroscopy can be utilized to study the chemical interaction and hybridization at the interface in such heterostructures.

## Data availability

The datasets used and/or analyzed during the current investigation are accessible from the corresponding author on reasonable request.

Received: 16 November 2023; Accepted: 11 February 2024

Published online: 01 March 2024

## References

1. Chhowalla, M. *et al.* The chemistry of two-dimensional layered transition metal dichalcogenide nanosheets. *Nat. Chem.* **5**, 263 (2013).
2. Han, S. A., Bhatia, R. & Kim, S.-W. Synthesis, properties and potential applications of two-dimensional transition metal dichalcogenides. *Nano Convergence* **2**, 17 (2015).
3. Sierra, J. F., Fabian, J., Kawakami, R. K., Roche, S. & Valenzuela, S. O. Van der Waals heterostructures for spintronics and opto-spintronics. *Nat. Nanotechnol.* **16**, 856 (2021).
4. Zhang, S. L. & Zhang, Z. *In Metallic Films for Electronic, Optical and Magnetic Applications* 244–301 (Woodhead Publishing, 2014).
5. Xie, Q. *et al.* Giant enhancements of perpendicular magnetic anisotropy and spin-orbit Torque by a MoS<sub>2</sub> layer. *Adv. Mater.* **31**, 1900776 (2019).
6. Zhou, Z. *et al.* Large perpendicular magnetic anisotropy in Ta/CoFeB/MgO on full-coverage monolayer MoS<sub>2</sub> and first-principles study of its electronic structure. *ACS Appl. Mater. Interfaces* **13**, 27 (2021).
7. Thiruvengadam, V., Mishra, A., Mohanty, S. & Bedanta, S. Anisotropy and domain structure in nanoscale-thick MoS<sub>2</sub>/CoFeB heterostructures: Implications for transition metal dichalcogenide-based thin films. *ACS Appl. Nano Mater.* **5**, 10645 (2022).
8. Yousef Vand, M., Jamilpanah, L., Zare, M. & Mohseni, S. M. Magnetic NiFe thin films composing MoS<sub>2</sub> nanostructures for spin-tropic application. *Sci. Rep.* **1**, 12 (2022).
9. Feng, N. *et al.* Magnetism by interfacial hybridization and p-type doping of MoS<sub>2</sub> in Fe<sub>4</sub>N/MoS<sub>2</sub> superlattices: A first-principles study. *ACS Appl. Mater. Interfaces* **6**, 6 (2014).
10. MacNeill, D. *et al.* Control of spin-orbit torques through crystal symmetry in WTe<sub>2</sub>/ferromagnet bilayers. *Nat. Phys.* **13**, 300 (2017).
11. Chun-I, L. *et al.* Spontaneously induced magnetic anisotropy in an ultrathin Co/MoS<sub>2</sub> heterojunction. *Nanoscale Horizons* **J. 5**, 1058 (2020).
12. Wang, W. *et al.* Spin-Valve Effect in NiFe/MoS<sub>2</sub>/NiFe Junction. *Nano Lett.* **15**, 5261 (2015).
13. Dastgeer, G. *et al.* Surface spin accumulation due to the inverse spin Hall effect in WS<sub>2</sub> crystals. *2D Mater.* **6**, 011007 (2018).
14. Dastgeer, G. *et al.* Gate modulation of the spin current in graphene/WS<sub>2</sub> van der Waals heterostructure at room temperature. *J. Alloy. Compd.* **919**, 165815 (2022).
15. Nisar, S. *et al.* Distinct detection of thermally induced spin voltage in Pt/WS<sub>2</sub>/Ni<sub>81</sub>Fe<sub>19</sub> by the inverse spin hall effect materials. *Today Nano* **24**, 100405 (2023).
16. Dastgeer, G., Shehzad, M. A. & Eom, J. Distinct detection of thermally induced spin voltage in Pt/WS<sub>2</sub>/Ni<sub>81</sub>Fe<sub>19</sub> by the inverse spin hall effect. *ACS Appl. Mater. Interfaces* **11**, 48533 (2019).
17. Hsu, C.-C. *et al.* Magnetic decoupling of Fe coverage across atomic step of MoS<sub>2</sub> flakes on SiO<sub>2</sub> surface. *J. Phys. D Appl. Phys.* **50**, 415001 (2017).
18. Tuli, F. J., Kibria, M. T., Nakagawa, T. & Mizuno, S. Interfacial magnetic behaviors and chemical states of Fe grown on MoS<sub>2</sub>. *Physica Status Solidi (B): Basic Research* **258**, 2100124 (2021).
19. Hsu, H.-C. *et al.* Surface morphology, magnetism and chemical state of Fe coverage on MoS<sub>2</sub> substrate. *Appl. Surf. Sci.* **357**, 551–557 (2015).
20. Garandel, T., Arras, R., Marie, X., Renucci, P. & Calmels, L. Electronic structure of the Co(0001)/MoS<sub>2</sub> interface and its possible use for electrical spin injection in a single MoS<sub>2</sub> layer. *Phys. Rev. B* **95**, 075402 (2017).
21. Yang, K.-Y. *et al.* Large area MoS<sub>2</sub> thin film growth by direct sulfurization. *Sci. Rep.* **13**, 8378 (2023).
22. Muratore, C., Voevodin, A. A. & Glavin, N. R. Physical vapor deposition of 2D Van der Waals materials: A review. *Thin Solid Films* **688**, 137500 (2019).
23. Chow, P. K. *et al.* Defect-induced photoluminescence in monolayer semiconducting transition metal dichalcogenides. *ACS Nano* **9**, 3 (2015).
24. Ghosh, S., Karmaker, S. C., Harish, S. & Saha, B. B. Atomic force microscopic investigations of MoS<sub>2</sub> thin films produced by low pressure sulfurization. *Micro Nanostruct.* **170**, 207400 (2022).
25. Park, J. *et al.* Comparison of hydrogen sulfide gas and sulfur powder for synthesis of molybdenum disulfide nanosheets. *Curr. Appl. Phys.* **16**, 691 (2016).
26. Li, J. *et al.* Magnetic dead layer at the interface between a Co film and the topological insulator Bi<sub>2</sub>Se<sub>3</sub>. *Phys. Rev. B* **86**, 054430 (2012).
27. Zehner, J. *et al.* Voltage-controlled deblocking of magnetization reversal in thin films by tunable domain wall interactions and pinning sites. *Adv. Electron Mater.* **6**, 2000406 (2020).
28. Hussain, Z., Raghavendra Reddy, V., Gupta, M., Srihari, V. & Pandey, K. K. Study of magnetic zigzag domain walls and magnetization reversal process in polycrystalline cobalt thin films: Effect of thickness and crystallographic texturing. *Thin Solid Films* **719**, 138492 (2021).

## Acknowledgements

Z.H. would like to thank Dr. V. Raghavendra Reddy and Dr. Mukul Gupta from UGC-DAE Consortium for Scientific Research for providing Kerr microscopy and D.C sputtering deposition techniques. The acknowledgment are extended to Dr. Ashish Waghmare and Prof. Sandesh Jadkar for helping us with sulfurization technique. SSP would like to thank Khalifa University for its financial support through the internal funds for high-quality

publications. Further, the authors extend their sincere appreciation to the Researchers Supporting Project number (RSP2024R370), King Saud University, Riyadh, Saudi Arabia, for the financial support.

### Author contributions

Z.H. investigation, analysis and wrote the manuscript. S.P. investigation and resources. S.S. resources P.E.L. resources H.M.P. project administration and resources. All the authors reviewed the manuscript.

### Competing interests

The authors declare no competing interests.

### Additional information

**Supplementary Information** The online version contains supplementary material available at <https://doi.org/10.1038/s41598-024-54316-1>.

**Correspondence** and requests for materials should be addressed to Z.H. or S.P.P.

**Reprints and permissions information** is available at [www.nature.com/reprints](http://www.nature.com/reprints).

**Publisher's note** Springer Nature remains neutral with regard to jurisdictional claims in published maps and institutional affiliations.



**Open Access** This article is licensed under a Creative Commons Attribution 4.0 International License, which permits use, sharing, adaptation, distribution and reproduction in any medium or format, as long as you give appropriate credit to the original author(s) and the source, provide a link to the Creative Commons licence, and indicate if changes were made. The images or other third party material in this article are included in the article's Creative Commons licence, unless indicated otherwise in a credit line to the material. If material is not included in the article's Creative Commons licence and your intended use is not permitted by statutory regulation or exceeds the permitted use, you will need to obtain permission directly from the copyright holder. To view a copy of this licence, visit <http://creativecommons.org/licenses/by/4.0/>.

© The Author(s) 2024